Active Viscoelastic Matter: From Bacterial Drag Reduction to Turbulent Solids

E. J. Hemingway,[1] A. Maitra,[2] S. Banerjee,[3,4] M. C. Marchetti,[3] S. Ramaswamy,[5,2] S. M. Fielding,[1] and M. E. Cates[6]
[1]Department of Physics, Durham University, Science Laboratories, South Road, Durham DH1 3LE, United Kingdom
[2]CCMT, Department of Physics, Indian Institute of Science, Bangalore 560 012, India
[3]Physics Department and Syracuse Biomaterials Institute, Syracuse University, Syracuse, New York 13244, USA
[4]James Franck Institute, University of Chicago, Chicago, Illinois 60637, USA
[5]TIFR Centre for Interdisciplinary Sciences, 21 Brundavan Colony, Osman Sagar Road, Narsingi, Hyderabad 500 075, India
[6]SUPA, School of Physics and Astronomy, University of Edinburgh, James Clerk Maxwell Building, Peter Guthrie Tait Road, Edinburgh EH9 3FD, United Kingdom
(Received 22 October 2014; published 5 March 2015)

A paradigm for internally driven matter is the active nematic liquid crystal, whereby the equations of a conventional nematic are supplemented by a minimal active stress that violates time-reversal symmetry. In practice, active fluids may have not only liquid-crystalline but also viscoelastic polymer degrees of freedom. Here we explore the resulting interplay by coupling an active nematic to a minimal model of polymer rheology. We find that adding a polymer can greatly increase the complexity of spontaneous flow, but can also have calming effects, thereby increasing the net throughput of spontaneous flow along a pipe (a "drag-reduction" effect). Remarkably, active turbulence can also arise after switching on activity in a sufficiently soft elastomeric *solid*.

DOI: 10.1103/PhysRevLett.114.098302 PACS numbers: 47.57.Lj, 61.30.Jf, 87.16.Ka, 87.19.rh

Active materials include bacterial swarms in a fluid, the cytoskeleton of living cells, and "cell extracts" containing only filaments, molecular motors, and a fuel supply [1–4]. Such materials are interesting because of their direct biophysical significance, and as representatives of a wider class of systems in which deviations from thermal equilibrium are not created by initial or boundary conditions (a temperature quench or motion of walls in a shear cell) but arise microscopically in the dynamics of each particle. By continually converting chemical energy into motion, active matter violates time-reversal symmetry, suspending the normal rules of thermal equilibrium dynamics (until the fuel runs out), causing strongly nonequilibrium features such as spontaneous flow. This flow may remain steady and laminar at the scale of the system, may show limit cycles at that scale or below, or may show spatiotemporal chaos. Since it resembles the inertial turbulence of a passive Newtonian fluid, the latter outcome is commonly called "bacterial" (or "active") turbulence [2,5–9]. The mechanism is quite distinct, however, stemming from a balance between active stress and orientational relaxation, rather than between inertia and viscosity as in conventional turbulence.

The phenomenology of activity-driven spontaneous flow can be understood, to a remarkable extent, using conceptually simple continuum models [1,10–12]. These start from the hydrodynamic equations of a passive fluid of rodlike objects with either polar [11] or nematic [12] local order, the latter characterized by a tensor order parameter $\mathbf{Q}(\mathbf{r})$ [12]. To the passive equations for such a liquid crystal (LC) [13] are then added leading-order violations of time-reversal symmetry; after a renormalization of passive parameters and allowing for fluid incompressibility, what remains is a bulk stress $\mathbf{\Sigma}_A = -\zeta\mathbf{Q}$ where ζ, an activity parameter, is positive for extensile systems, negative for contractile. In extensile materials each rodlike particle pulls fluid inwards equatorially and emits it symmetrically from the poles, with the reverse for the contractile case. Even without accurate knowledge of ζ, this approach makes for robust predictions. For example, extensile and contractile systems become separately unstable toward spontaneous flow states at critical activity levels that are system-size dependent and that vanish for bulk samples. Numerical solutions of the active nematic equations [5,7–9] show spontaneous flows resembling experiments on bacterial swarms [2] and on microtubule-based cell extracts [4]. Both of these are extensile nematics, and we restrict ourselves to this case below [14].

Active nematogenic fluids are often referred to as "active gels" [5,11]. But, although all LCs are somewhat viscoelastic (due to slow defect motion), these models assume fast local relaxations and mostly do not address gels in a conventional sense [15]. Certainly they do not capture the diversity of viscoelastic behavior that one expects in subcellular active matter containing long-chain flexible polymers, or other cytoplasmic components, with long (possibly divergent) intrinsic relaxation times. These slow relaxations should couple to the orientational order, strongly modifying the effects of activity. Polymers could also play a strong role in modifying diffusion [16] and active flows at the supracellular level: they are present in mucus, saliva, and other viscoelastic fluids in which swarms of motile bacteria reside. Notably, many bacteria excrete their own polymers [17], suggesting an advantage in controlling the viscoelasticity of their surroundings.

In this Letter, therefore, we present a model that addresses the interplay between active LCs and polymers [15]. We sketch its derivation (which requires care) and give examples of its rich dynamics (which will be explored further in [18]). Highlights include an exotic form of "drag reduction" by polymers for active (noninertial) turbulence, spontaneous flows with slow polymer-driven oscillations, and transient active turbulence within a material that is ultimately a solid.

The symmetric and antisymmetric parts of the center-of-mass velocity-gradient tensor $(\nabla \mathbf{v})_{ij} \equiv \partial_i v_j$ are denoted by $\mathbf{D}$ and $\mathbf{\Omega}$ [19]. For other tensors the symmetric, antisymmetric, and traceless parts carry superscripts S, A, and T. Conformation tensors for the polymer and the LC are denoted by $\mathbf{C}$ and $\mathbf{Q}$, where $\mathbf{Q}$ is traceless. The polymeric tensor is $\mathbf{C} = \langle \mathbf{rr} \rangle$, where $\mathbf{r}$ is the end-to-end vector of a chain (or subchain, depending on the level of description). We introduce a free energy density $f = f_Q(\mathbf{Q}, \nabla \mathbf{Q}) + f_C(\mathbf{C}) + f_{QC}(\mathbf{Q}, \mathbf{C})$ where f_Q and f_C are standard forms for active nematics [13] and dumbbell polymers [20], respectively, as detailed in Ref. [21]. The lowest order passive coupling is

$$f_{QC} = \kappa \mathrm{Tr}[\mathbf{C} - \mathbf{I}]\mathrm{Tr}[\mathbf{Q}^2] + 2\chi \mathrm{Tr}[\mathbf{CQ}]. \tag{1}$$

Both terms vanish for undeformed polymers ($\mathbf{C} = \mathbf{I}$).

From the free energy $F = \int f dV$ we next derive the nematic molecular field $\mathbf{H} \equiv -(\delta F/\delta \mathbf{Q})^{ST}$ as

$$\mathbf{H} = -G_Q \left[\left(1 - \frac{\gamma}{3}\right)\mathbf{Q} - \gamma \mathbf{Q}^2 + \gamma \mathbf{Q}^3 \right] - G_Q \gamma \frac{\mathbf{I}}{3} \mathrm{Tr}[\mathbf{Q}^2] + K \nabla^2 \mathbf{Q} - 2\kappa \mathrm{Tr}[\mathbf{C} - \mathbf{I}]\mathbf{Q} - 2\chi \mathbf{C}^T. \tag{2}$$

Here G_Q is a bulk free energy density scale set by f_Q, K the nematic elastic constant, γ a control parameter for the nematic transition, and G_C the polymer elastic modulus. (See the details in Ref. [21].) The corresponding molecular field for polymer conformations is simpler: $\mathbf{B} \equiv -(\delta F/\delta \mathbf{C}) = -G_C(\mathbf{I} - \mathbf{C}^{-1})/2 - \kappa \mathbf{I} \mathrm{Tr}[\mathbf{Q}^2] - 2\chi \mathbf{Q}$.

The most general equations of motion then involve at least four separate fourth-rank tensors describing how $\mathbf{Q}$ and $\mathbf{C}$ respond to these molecular fields, and to imposed velocity gradients. For simplicity we choose the response tensors of the Beris-Edwards LC theory and the Johnson-Segalman (JS) polymer model, respectively [13]. We then allow for conformational diffusion in the polymer sector [26], which adds a gradient term in $\mathbf{C}$ of kinetic origin [21]. The result is a minimally coupled model of the passive $\mathbf{C} + \mathbf{Q}$ dynamics that reduces to well-established models when either order parameter is suppressed.

To the coupled passive model we finally add a minimal set of active terms [12]. In principle one can add all terms that violate time-reversal symmetry arising at zeroth order in gradients and first order in either $\mathbf{Q}$ or $\mathbf{C} - \mathbf{I}$; these are given in Ref. [21]. Here we suppose, for simplicity, that the polymers are not themselves active and respond to nematic activity only through fluid advection. This captures the effect of adding polymer to (say) a cell extract; alternatively, this could describe the collective dynamics of bacterial suspensions in mucus. (In contrast, one could build a system of polymers directly from active elements [27].) There remain two active terms linear in $\mathbf{Q}$; one can be absorbed into f_Q, and the other is the familiar active deviatoric stress $\mathbf{\Sigma}_A = -\zeta \mathbf{Q}$ [12].

The resulting equations of motion for $\mathbf{Q}$ and $\mathbf{C}$ are

$$(\partial_t + \mathbf{v} \cdot \nabla)\mathbf{Q} = \mathbf{Q\Omega} - \mathbf{\Omega Q} + \frac{2\xi}{3}\mathbf{D} + 2\xi[\mathbf{QD}]^{ST} - 2\xi \mathbf{Q} \mathrm{Tr}[\mathbf{QD}] + \tau_Q^{-1}\mathbf{H}/G_Q, \tag{3}$$

$$(\partial_t + \mathbf{v} \cdot \nabla)\mathbf{C} = \mathbf{C\Omega} - \mathbf{\Omega C} + 2a[\mathbf{CD}]^S + \tau_C^{-1}(2[\mathbf{BC}]^S/G_C + \ell_C^2 \nabla^2 \mathbf{C}). \tag{4}$$

Here ξ is the flow-alignment parameter of the nematic [28] and a is the slip parameter of the JS model. Each controls the relative tendency of molecules to align with streamlines and rotate with local vorticity. Parameters τ_Q, τ_C are the intrinsic relaxation times for the nematic and the polymer, while ℓ_C governs diffusion in the JS sector [26].

The incompressible fluid velocity $\mathbf{v}$ obeys the Navier-Stokes equation $\rho(\partial_t + v_\beta \partial_\beta)v_\alpha = \partial_\beta(\Sigma_{\alpha\beta})$, whose stress $\mathbf{\Sigma} = -P\mathbf{I} + 2\eta \mathbf{D} + \mathbf{\Sigma}_A + \mathbf{\Sigma}_Q + \mathbf{\Sigma}_C$ combines an isotropic pressure P, a contribution from a Newtonian solvent of viscosity η, and the active stress $\mathbf{\Sigma}_A$ with two reactive stresses [29]:

$$\mathbf{\Sigma}_Q = -K(\nabla \mathbf{Q}) : (\nabla \mathbf{Q}) + 2[\mathbf{QH}]^A - \frac{2\xi}{3}\mathbf{H} - 2\xi[\mathbf{QH}]^{ST} + 2\xi \mathbf{Q} \mathrm{Tr}[\mathbf{QH}], \tag{5}$$

$$\mathbf{\Sigma}_C = -2a[\mathbf{CB}]^S + 2[\mathbf{CB}]^A. \tag{6}$$

Crucially, ξ and a must appear as shown in the reactive stresses to recover a correct passive limit [13]. In the pure JS case—but not in general—one can absorb the factor a in Eq. (6) into G_C, restoring consistency to the classical JS model, which sets $\mathbf{\Sigma}_C = -2\mathbf{BC}$ for all a [13,30]. A less careful marriage of JS with active nematic theory would thus have set $a = 1$ in Eq. (6) but not Eq. (4), violating thermodynamic principles [31] and giving incorrect physics.

We choose ξ and a within the flow-aligning and outwith the shear-banding ranges of their respective models, to avoid tumbling and banding instabilities of the passive model in flow. We neglect inertia ($\rho = 0$) and choose units where $G_Q = \tau_Q = L_y = 1$, with L_y the width of the sample, a 2D simulation box of $L_x \times L_y = 4 \times 1$. We choose periodic boundary conditions in x, with no slip (of $\mathbf{v}$) and no gradient (of $\mathbf{Q}$ or $\mathbf{C}$) at the sample walls ($y = 0, L_y$). Default values for numerics are $\xi = 0.7$, $\eta = 0.567$, and $\gamma = 3$ (directly comparable to Ref. [5] for the polymer-free case); we set $a = 1$. We vary τ_C over several decades $10^{-2} \leq \tau_C \leq 10^6$ at fixed polymer viscosity

$\eta_C \equiv \tau_C G_C = 1$, allowing for fast or slow relaxation while retaining the comparability of $\mathbf{\Sigma}_{Q,C}$. We define $\ell_Q = (K/G_Q)^{1/2}$, the Frank length for nematic distortions, and vary this in the range $0.002 \leq \ell_Q/L_y \leq 0.025$ (comparable to other studies [5,6]), then set $\ell_C^2/\tau_C = \ell_Q^2/\tau_Q$ to equate the diffusivities of $\mathbf{Q}$ and $\mathbf{C}$. Using careful numerics we are able to address several decades of activity level $10^{-4} \leq \zeta \leq 6$. Finally, most of our work addresses the simplest case, where the coupling of $\mathbf{Q}$ and $\mathbf{C}$ is purely kinematic: i.e., $\kappa = \chi = 0$. In this limit, interaction between the polymer and $\mathbf{Q}$ is indirect, mediated only via the background fluid velocity $\mathbf{v}$. However we also present some results for nonzero χ, as arises in passive nematic elastomers [32].

First, with kinematic coupling only, we ask whether the addition of a polymer can suppress the intrinsic instability of active nematics towards bulk flow. Generalizing previous results [5,11,33,34], a linear stability analysis (detailed in Ref. [21]) allowing 1D perturbations of wave vector $\mathbf{k}$ about the quiescent nematic base state gives a critical activity level (for $\gamma = 3$)

$$\zeta_c = \frac{12k^2\ell_Q^2}{\Lambda\tau_Q}\left(\eta + \frac{\Lambda^2 G_Q \tau_Q}{72} + \frac{a^2\eta_C}{1+k^2\ell_C^2}\right), \qquad (7)$$

where $\Lambda = 5\xi \pm 3$ for $\mathbf{k}$ perpendicular $(-)$ or parallel $(+)$ to the major axis of $\mathbf{Q}$. Thus ζ_c always vanishes in bulk (as $k \to 0$), while the final term shows the stabilizing effect of polymer in finite systems. This effect is viscous and not viscoelastic in character since at threshold, the time scale for growth diverges, with τ_C then infinitely fast in comparison. This analysis, which we have confirmed numerically (Fig. 1), contrasts with Ref. [16], which reports polymer-induced bulk stabilization for a related but distinct active model (with no inherent nematic tendency).

Figure 1 shows phase diagrams on the ζ, Δ plane, where $\Delta \equiv (\ell_Q/L_y)^2$ represents the stabilizing effect of small sample sizes. Varying τ_C at a fixed $\eta_C = 1$ reveals a very interesting effect of strictly viscoelastic origin. Among the states showing active turbulence, adding a polymer significantly extends the parameter range in which macroscopic symmetry is broken (the filled symbols in Fig. 1), as judged by a criterion (see Ref. [21]) of significant net throughput of fluid along the (periodic) x direction. Thus adding a polymer to (say) a fluid showing bacterial turbulence should effectively "reduce drag" by enhancing throughput at fixed (active) stress—as it does for pressure-driven turbulent pipe flow in a passive fluid [36]. The polymer calms the short scale structure of the active flow, decreasing the nematic defect density and increasing the flow correlation length towards the system size, thereby favoring restoration of a more organized flow state.

This calming effect of a polymer on active flow can be reversed by adding direct coupling alongside the kinematic one. Of the two couplings in f_{QC}, only the χ term is sensitive to the relative orientation of tensors $\mathbf{C}$ and $\mathbf{Q}$; the disruptive case is $\chi > 0$, so that these tensors want to be misaligned. Figure 2 shows three novel flow states; for movies see Ref. [37]. Among these are a shear banded state with interfacial defects (related to those seen in [8,38]), coexistence of "bubbling" active domains and regions with director along the vorticity axis, and states showing periodic modulation of a complex flow pattern on a long time scale set by τ_C, confirming a direct role for polymer viscoelasticity in creating these new states.

New and unexpected physics can also arise when this long polymeric time scale becomes effectively infinite, as would describe an active nematic (such as an actomyosin cell extract) within a background of a lightly cross-linked elastomer. We address this limit in two ways: first by

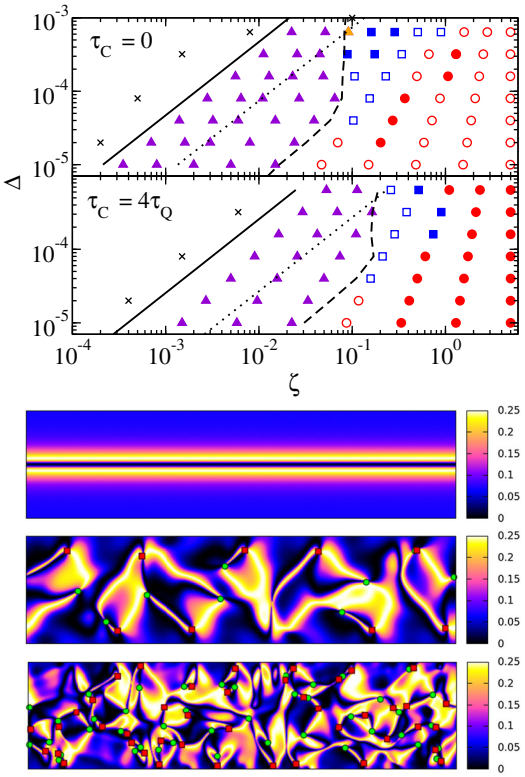

FIG. 1 (color online). State diagrams without (upper panels) and with (lower panels) a polymer of relaxation time $\tau_C = 4\tau_Q$. The initial condition is director $\mathbf{n}$ (i.e., the major axis of $\mathbf{Q}$), uniformly along y. Symbols are ×: quiescent, squares: oscillatory, triangles: steady banded flow (cf. Refs. [5,35]), circles: unsteady or chaotic. Filled symbols denote states with a significant net throughput (along the periodic direction x). Solid lines show the 1D instability (the bending mode) of the specified initial condition, dotted lines the splay mode for the initial condition with $\mathbf{Q}$ along x, and dashed lines the observed crossover line $\zeta_c^{\text{bend 2D}}$ beyond which the phase diagram becomes independent of which of these initial states was chosen. The bottom three panels show states, all with net throughput, from the $\tau_C = 4$ phase diagram above: banded ($\zeta = 0.023$, $\Delta = 10^{-5}$), oscillatory ($\zeta = 0.741$, $\Delta = 1.6 \times 10^{-4}$), and chaotic ($\zeta = 1.75$, $\Delta = 8 \times 10^{-5}$); the color scale indicates $(n_x n_y)^2$. Defects of topological charge $\pm 1/2$ are identified by green dots $(+)$ and red squares $(-)$.

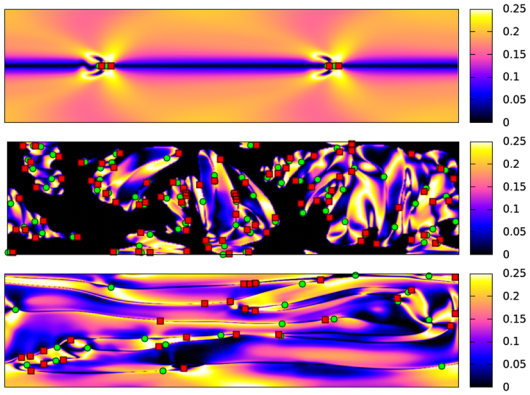

FIG. 2 (color online). Three spontaneous flow states seen with added polymer, all with $\tau_C = 10$. (Upper panel) A pair of defects traveling along the interface of a shear-banded state ($\zeta = 3.2$, $\Delta = 10^{-4}$, $\chi = 0.002$). (Middle panel) Coexistence of bubbling active domains and regions where the director is out of plane (black) ($\zeta = 6, \Delta = 10^{-4}, \chi = 0.004$). (Lower panel) An exotic oscillatory state which coherently "shuffles" left and right on time scale τ_C ($\zeta = 6$, $\Delta = 10^{-4}$, $\chi = 0.002$). The color scale indicates $(n_x n_y)^2$.

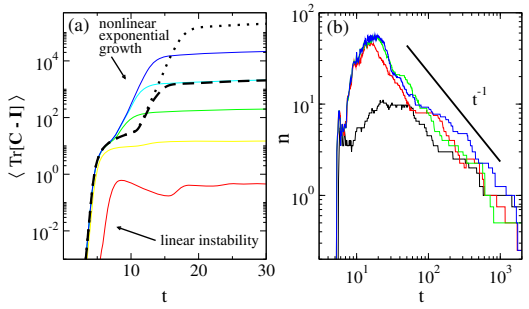

FIG. 3 (color online). (a) A scalar measure of polymer stress, $\langle \mathrm{Tr}[\mathbf{C} - \mathbf{I}] \rangle$, against time for $\tau_C = 10^0$(bottom, red line) $\rightarrow 10^4$ (top, blue line) at a fixed $\eta_C = 1$. Data for τ_C infinite, $G_C = 10^{-3}$ (bold dashed line), 10^{-5} (bold dotted line) are also shown. (b) Areal defect density n against time for infinite τ_C, with $G_C = 10^{-1}$(black, bottom line) $\rightarrow 10^{-7}$ (blue, top line); steps arise because n is discrete. In both panels, $\zeta = 3.2$, $\Delta = 8 \times 10^{-5}$.

increasing τ_C (holding $\eta_C = 1$), then with τ_C infinite at small finite G_C (giving infinite η_C). The passive limit of this system is a nematic elastomer [32]; a full theoretical treatment of the active counterpart will be presented elsewhere [39]. One might expect all of the flow instabilities reported above to be completely absent in what is, after all, a solid material, but this expectation turns out to be misleading. Since $G_C \ll G_Q$, the sample can strongly deform before its small elastic modulus has appreciable effects [40]. Accordingly the system should initially show a spontaneous flow instability as though no polymer were present, possibly allowing complex LC textures to form, which then must respond to a growing polymer stress. Numerically (setting $\chi = 0$ for simplicity) we indeed find the onset of spontaneous flow. For $\tau_C \lesssim \tau_Q = 1$ the dynamics is essentially the same as without a polymer, and the exponential growth of a shear banding instability is tracked by the polymer stress. We have checked that these observations are stable for small, negative values of χ.

Strikingly, for $\tau_C \gtrsim \tau_Q$, the first phase of exponential growth is followed by a second one [Fig. 3(a)], arising because the active turbulent state—like its passive inertial counterpart—contains regions of extensional flow where polymers stretch strongly in time. Although for small G_C large local strains are needed to arrest the spontaneous flow, the time needed to achieve these grows only logarithmically as $G_C \rightarrow 0$. For $\tau_C \gg \tau_Q$, rather soon after its initial formation, the turbulent state indeed arrests into a complex but almost frozen defect pattern. Thereafter the defect density decays slowly, roughly as t^{-1} [see Fig. 3(b) for the $\tau_C \rightarrow \infty$ case], which is the classical result for passive nematic coarsening [41]. This process is slow enough that the strain pattern created by the arrested active turbulence might easily be mistaken for a final steady state. Our arrest mechanism, where strong polymer stretching in extensional flow regions creates strong stresses in opposition, may relate closely to the drag reduction effects reported above.

To address active viscoelastic matter, we have created a continuum model combining the theory of active nematics with the well-established JS model of polymers. In the passive limit, our model is thermodynamically admissible by design—a nontrivial achievement since the JS model itself is admissible only by accident. Our model shows that polymers can shift, but not destroy, the generic instability to spontaneous flow shown by active nematics above a critical activity (which still vanishes for large systems). They can also have a strong bacterial drag reduction effect, promoting finite throughput in states of active turbulence.

An antagonistic coupling between polymer and nematic orientations produces instead new and complex spontaneous flows, some with oscillation periods set by the polymer relaxation time. Finally, the elastomeric limit of our model reveals, strikingly, that classifying a material as a solid does not *a priori* preclude its showing turbulent behavior. Though implausible for inertial turbulence, in the active case this outcome, which arises when $G_C/G_Q \lesssim 0.1$, looks experimentally feasible for subcellular active matter (though probably not swarms of bacteria) within a lightly cross-linked polymer gel. We hope our work will promote experiments on these and other forms of active viscoelastic matter.

We thank Peter Olmsted for illuminating discussions. E. J. H. thanks EPSRC for a studentship. M. E. C. thanks EPSRC (Grant No. J007404) and the Royal Society for funding. The research leading to these results has received funding (S. M. F.) from the European Research Council under the European Union's Seventh Framework Programme (FP7/2007–2013)/ERC Grant Agreement No. 279365. S. R. acknowledges a J. C. Bose Fellowship of the DST, India and A. M. thanks TCIS, TIFR for their hospitality. M. C. M. was supported by the National Science Foundation through Grants No. DMR-1305184 and No. DGE-1068780 and by the Simons Foundation. The authors thank the KITP at the University of California,

Santa Barbara, where they were supported through National Science Foundation Grant No. NSF PHY11-25925 and Gordon and Betty Moore Foundation Grant No. 2919.

Note added.—Recently, a paper appeared addressing similar topics from a somewhat different perspective [42]. This treats the spontaneous flow of active particles embedded in a viscoelastic fluid in two dimensions, but unlike our work it (a) omits liquid-crystalline order and (b) allows for concentration fluctuations. This complementary approach qualitatively confirms some of our findings on bacterial drag reduction.

[1] M. C. Marchetti, J.-F. Joanny, S. Ramaswamy, T. B. Liverpool, J. Prost, M. Rao, and R. A. Simha, Rev. Mod. Phys. **85**, 1143 (2013).

[2] C. Dombrowski, L. Cisneros, S. Chatkaew, R. E. Goldstein, and J. O. Kessler, Phys. Rev. Lett. **93**, 098103 (2004).

[3] F. J. Nédélec, T. Surrey, A. C. Maggs, and S. Leibler, Nature (London) **389**, 305 (1997).

[4] T. Sanchez, D. T. N. Chen, S. J. DeCamp, M. Heymann, and Z. Dogic, Nature (London) **491**, 431 (2012).

[5] S. M. Fielding, D. Marenduzzo, and M. E. Cates, Phys. Rev. E: Stat., Nonlinear, Soft Matter Phys. **83**, 041910 (2011).

[6] H. H. Wensink, J. Dunkel, S. Heidenreich, K. Drescher, R. E. Goldstein, H. Löwen, and J. M. Yeomans, Proc. Natl. Acad. Sci. U.S.A. **109**, 14308 (2012).

[7] L. Giomi, M. J. Bowick, X. Ma, and M. C. Marchetti, Phys. Rev. Lett. **110**, 228101 (2013).

[8] L. Giomi, M. J. Bowick, P. Mishra, R. Sknepnek, and M. C. Marchetti, Phil. Trans. R. Soc. A **372**, 20130365 (2014).

[9] S. P. Thampi, R. Golestanian, and J. M. Yeomans, Phys. Rev. Lett. **111**, 118101 (2013).

[10] S. Ramaswamy, Annu. Rev. Condens. Matter Phys. **1**, 323 (2010).

[11] R. Voituriez, J.-F. Joanny, and J. Prost, Europhys. Lett. **70**, 404 (2005).

[12] R. A. Simha and S. Ramaswamy, Phys. Rev. Lett. **89**, 058101 (2002).

[13] A. N. Beris and B. J. Edwards, *Thermodynamics of Flowing Systems* (Oxford University Press, Oxford, 1994).

[14] By contrast, actomyosin systems, including the cytoskeleton, are typically contractile and polar; see F. Jülicher, K. Kruse, J. Prost, and J.-F. Joanny, Phys. Rep. **449**, 3 (2007).

[15] A. C. Callan-Jones and F. Jülicher, New J. Phys. **13**, 093027 (2011) considers true multicomponent active gels, but does not explore rheology; a related but distinct combination of activity and viscoelasticity has been used to address tissue dynamics; see J.-F. Joanny and J. Prost, Séminaire Poincaré **XII**, 1 (2009); J. Ranft, M. Basan, J. Elgeti, J.-F. Joanny, J. Prost, and F. Jülicher, Proc. Natl. Acad. Sci. U.S.A. **107**, 20863 (2010); see also C. Storm, J. J. Pastore, F. C. MacKintosh, T. C. Lubensky, and P. A. Janmey, Nature (London) **435**, 191 (2005) for work addressing nonlinear polymer elasticity in active matter without the direct construction of a coupled model; see Ref. [16] below for a study along similar lines to ours but addressing individual active particles, not an active nematic continuum, within a linear viscoelastic medium.

[16] Y. Bozorgi and P. T. Underhill, J. Rheol. **57**, 511 (2013).

[17] A. W. Decho, Oceanogr. Mar. Biol. Annu. Rev **28**, 73 (1990).

[18] E. J. Hemingway, M. E. Cates, and S. M. Fielding (to be published).

[19] Reversing the order of indices in $\nabla \mathbf{v}$ would require a sign reversal of $\mathbf{\Omega}$ wherever it appears.

[20] S. T. Milner, Phys. Rev. E: Stat., Nonlinear, Soft Matter Phys. **48**, 3674 (1993).

[21] See Supplemental Material at http://link.aps.org/supplemental/10.1103/PhysRevLett.114.098302, which includes Refs. [22–25], for a description of the free energy structure, an enumeration of all possible leading-order active terms, and an outline of the stability analysis and throughput definition that we adopt.

[22] D. Marenduzzo, E. Orlandini, and J. M. Yeomans, Phys. Rev. Lett. **98**, 118102 (2007).

[23] P. D. Olmsted and C.-Y. D. Lu, Phys. Rev. E: Stat., Nonlinear, Soft Matter Phys. **60**, 4397 (1999).

[24] H. Pleiner, M. Liu, and H. R. Brand, Rheol. Acta **41**, 375 (2002).

[25] E. Bertin, H. Chaté, F. Ginelli, S. Mishra, A. Peshkov, and S. Ramaswamy, New J. Phys. **15**, 085032 (2013).

[26] P. D. Olmsted, O. Radulescu, and C.-Y. D. Lu, J. Rheol. **44**, 257 (2000).

[27] G. Jayaraman, S. Ramachandran, S. Ghose, A. Laskar, M. S. Bhamla, P. B. Sunil Kumar, and R. Adhikari, Phys. Rev. Lett. **109**, 158302 (2012).

[28] H. Stark and T. C. Lubensky, Phys. Rev. E: Stat., Nonlinear, Soft Matter Phys. **67**, 061709 (2003).

[29] The colon in Eq. (5) denotes contraction over the second and third Cartesian indices.

[30] P. D. Olmsted (private communication).

[31] H. C. Öttinger, *Beyond Equilibrium Thermodynamics* Wiley, New York, 2004).

[32] M. Warner and E. M. Terentjev, *Liquid Crystal Elastomers* (Oxford University Press, Oxford, 2002).

[33] S. A. Edwards and J. M. Yeomans, Europhys. Lett. **85**, 18008 (2009).

[34] L. Giomi, L. Mahadevan, B. Chakraborty, and M. F. Hagen, Nonlinearity **25**, 2245 (2012).

[35] M. E. Cates, S. M. Fielding, D. Marenduzzo, E. Orlandini, and J. M. Yeomans, Phys. Rev. Lett. **101**, 068102 (2008).

[36] C. M. White and M. G. Mungal, Annu. Rev. Fluid Mech. **40**, 235 (2008).

[37] See Supplemental Material at http://link.aps.org/supplemental/10.1103/PhysRevLett.114.098302 for movies of flowing states showing the principle eigenvalue of $\mathbf{Q}$ (color scale), director $\mathbf{n}$ (red lines), and $\pm\frac{1}{2}$ defects (green and red circles).

[38] S. P. Thampi, R. Golestanian, and J. M. Yeomans, Europhys. Lett. **105**, 18001 (2014).

[39] S. Banerjee, A. Maitra, M. C. Marchetti, S. Ramaswamy, and J. Toner (to be published).

[40] For a somewhat similar situation involving polymer glasses, see S. M. Fielding, R. G. Larson, and M. E. Cates, Phys. Rev. Lett. **108**, 048301 (2012).

[41] A. J. Bray, Adv. Phys. **43**, 357 (1994).

[42] Y. Bozorgi and P. T. Underhill, J. Non-Newtonian Fluid Mech. **214**, 69 (2014).